ISBN: 978-3-95450-233-2 ISSN: 2673-5504 doi:10.18429/JACoW-SRF2021-SUPFDV015

PRELIMINARY RESULTS FROM MAGNETIC FIELD SCANNING SYSTEM FOR A SINGLE CELL NIOBIUM CAVITY*

I. Parajuli†, J. Delayen, and A. Gurevich
Department of Physics, Old Dominion University, Norfolk, VA, USA
G. Ciovati[2], Thomas Jefferson National Accelerator Facility, Newport News, VA, USA
[2]also at Department of Physics, Old Dominion University, Norfolk, VA, USA

Abstract

One of the building blocks of modern particle accelerators is superconducting radiofrequency (SRF) cavities. Niobium is the material of choice to build such cavities, which operate at liquid helium temperature (2 - 4 K) and have some of the highest quality factors found in Nature. There are several sources of residual rf losses, one of them is trapped magnetic flux, which limits the quality factor in SRF cavities. The flux trapping mechanism depends on different niobium surface preparations and cool-down conditions. Suitable diagnostic tools are not yet available to study the effects of such conditions on magnetic flux trapping. A magnetic field scanning system (MFSS) for SRF cavities using Hall probes and fluxgate magnetometer has been designed, built, and it is commissioned to measure the local magnetic field trapped in 1.3 GHz single-cell SRF cavities at 4 K. In this contribution, we will present the preliminary results from MFSS for a single cell niobium cavity.

INTRODUCTION

Modern particle accelerators depend more and more on superconducting radio frequency (SRF) cavities because of their excellent efficiency, compared to the normal-conducting cavities. More than four decades of research and development has proven that bulk Niobium is the material of choice to build SRF cavities, which are used in modern particle accelerator. With the advancement in research and development of SRF cavities, the quality factor (Q_0) of SRF cavities is now routinely in range of 10^{10} to 10^{11} at 2 K with peak surface magnetic field of up to ≈200 mT [1, 2]. For high energy particle accelerator, we would like to have SRF cavities with higher accelerating gradient > 50 MV/m and a higher quality factor of $>10^{10}$. It is really challenging to fabricate a cavity with both high-quality factor and accelerating gradient due to RF losses in SRF cavities. Theoretically, when a superconducting cavities cool-down through the critical temperature (T_c), all magnetic flux lines should be expelled from the cavity. However, material defects such as dislocation, impurity precipitates, and grain boundaries are effective pinning sites where magnetic flux lines could get trap during cool-down through T_c.

Magnetic flux trapping is a leading cause of residual losses in superconducting Nb cavities, and it depends on cool-down conditions, surface preparation and ambient magnetic field [3-6]. Suitable diagnostic tools are in high demand to study the effects of such conditions on magnetic flux trapping to enhance cavity performance [7, 8]. We have designed, developed, and commissioned a magnetic field scanning system (MFSS) to detect trapped flux over a large fraction of the surface of 1.3 GHz single-cell cavities. In this contribution, we report initial results of the newly commissioned MFSS, which used cryogenic Hall probes (HP) and fluxgate magnetometers (FGM) to measure the trapped flux on the cavity surface at different cool-down conditions and different ambient magnetic field.

EXPERIMENTAL SETUP AND PROCEDURE

Experimental Setup

Figure 1 shows the assembled MFSS on a 1.3 GHz niobium SRF cavity. This setup consists of four HPs in one bracket and four FGMs in another bracket, 180° apart. The setup is developed in such a way that both brackets along with sensors can move from 0° to 360° in azimuthal direction, around the cavity axis. More detail about the magnetic field scanning system setup can be found in reference [9]. Figure 2 shows the orientation of the sensors with respect to the cavity axis. In order to measure the external applied magnetic field, we installed three fluxgate magnetometers FGMA, FGMB and FGMC. We used four Cernox temperature sensors, two at top beam tube labelled *a* and *b*, and two at the bottom beam tube labelled *c* and *d*, to measure the temperature at the cavity surface at four locations, T_a, T_b, T_c, T_d.

Experimental Procedure

A single-cell TESLA-shape 1.3 GHz niobium cavity labelled PJ1-1 was used for this study. The cavity, under vacuum, with the MFSS was inserted in a vertical cryostat at Jefferson Lab. We applied the certain amount of external magnetic field along the cavity axis using the compensation coils around the Dewar and we measured the applied field using three fluxgate magnetometers. We performed the experiment in two modes: “monitor mode” and “scan mode”.

In monitor mode, we kept all the sensors at a fixed location (no movement in the azimuthal direction) and performed a “fast cool-down” ($\leftrightarrows T$ across the cavity of ~20 K) through T_c. During fast cool-down, we recorded the magnetic field measured by four Hall probes using Aeropoc’s data acquisition module USB2ad. We also recorded the magnetic field measured by four fluxgate magnetometers

* Work supported by NSF Grant 100614-010. Work at Jefferson Lab is supported by Jefferson Science Associates, LLC under U.S. DOE Contract No. DE-AC05-06OR23177.
† Ipara001@odu.edu

ISBN: 978-3-95450-233-2 ISSN: 2673-5504 doi:10.18429/JACoW-SRF2021-SUPFDV015

using a single Mag01H module and a Keithley multiplexing module (2701/7701).

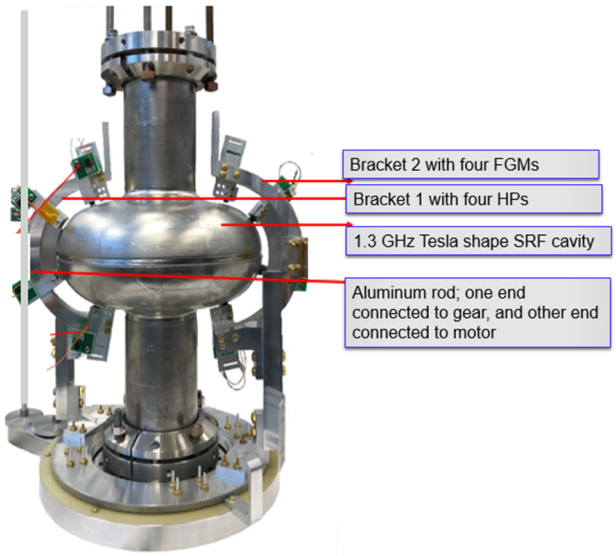

MFSS assembled on 1.3 GHz SRF cavity.

Figure 1: MFSS assembled on 1.3 GHz SRF cavity.

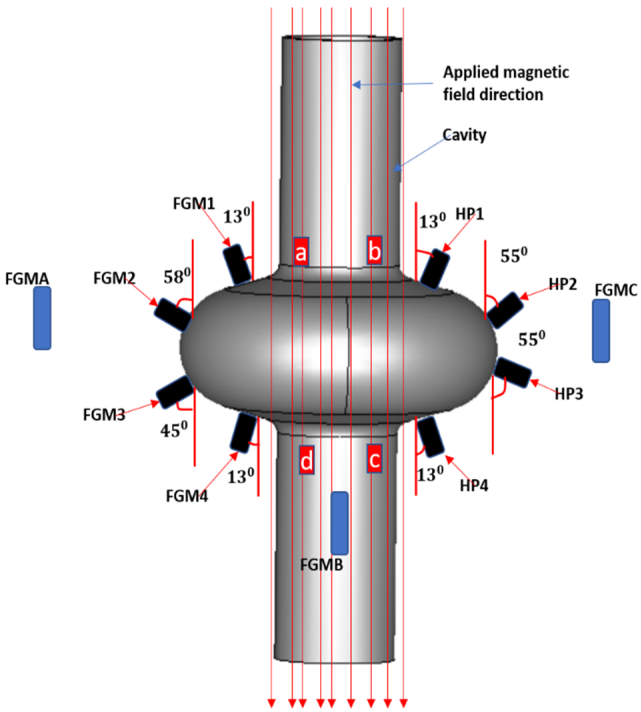

Figure 2: Schematic diagram of magnetic field sensors orientation.

In scan mode, initially we kept all sensor at the start position of 0° azimuthal angle. We measured the field with four Hall probes and then with the four fluxgate magnetometers. After that, we moved the sensors by 10° azimuthal angle and repeated the magnetic field measurement by HPs and FGMs. We repeated this process until we reached 360° azimuthal position. We also record the azimuthal position after each movement.

TEST RESULTS

Figure 3 shows the magnetic field measured by fluxgate magnetometers during fast cool-down. The magnetic field measured by the four fluxgate magnetometers is different since their orientation is different with respect to the cavity axis. Similarly, Figure 4 shows the magnetic field measured by Hall probes during fast cool-down. During this test, we applied ~240 mG of external magnetic field which has ~15° from cavity axis.

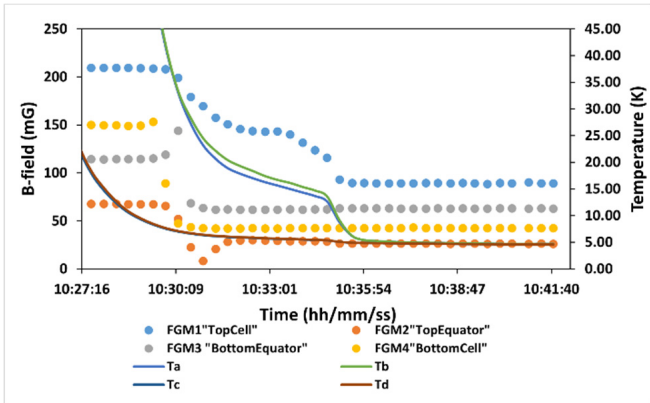

Figure 3: Magnetic field measured by fluxgate magnetometers vs time, and temperature vs time during monitor mode scan, during fast cool-down.

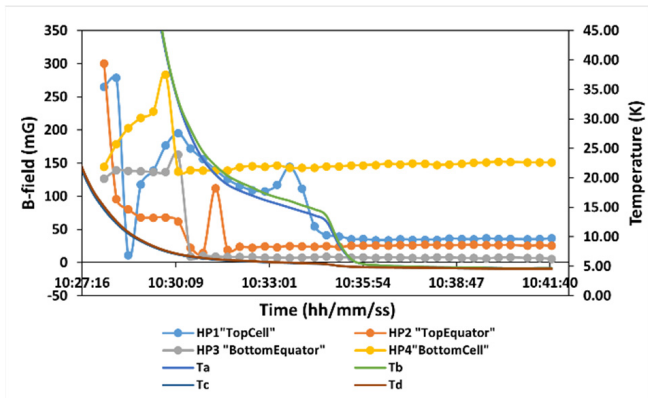

Figure 4: Magnetic field measured by fluxgate magnetometers vs time, and temperature vs time during monitor mode scan, during fast cool-down.

Figure 5 shows the magnetic field measured by FGMs and HPs with changing azimuthal position of probes. Before performing the magnetic field scanning, we applied external magnetic field of nearly 240 mG, and we cooled the cavity to 12 K. When cavity's temperature reached to 12 K, we kept external field as it is, and we per formed the scan mode test. Figure 6 shows the magnetic field versus azimuthal position of magnetic sensors. Before performing this test, we applied external magnetic field of ~240 mG and we did "slow" cool-down through T_c ($\leftrightarrows T$ across the cavity of ~0.2 K). Once the temperature of the cavity reached to 4 K, we lowered the external magnetic field to ~2 mG. Thus, the curves shown in Fig. 6 represent a measurement of the trapped magnetic field in the cavity wall.

ISBN: 978-3-95450-233-2 ISSN: 2673-5504 doi:10.18429/JACoW-SRF2021-SUPFDV015

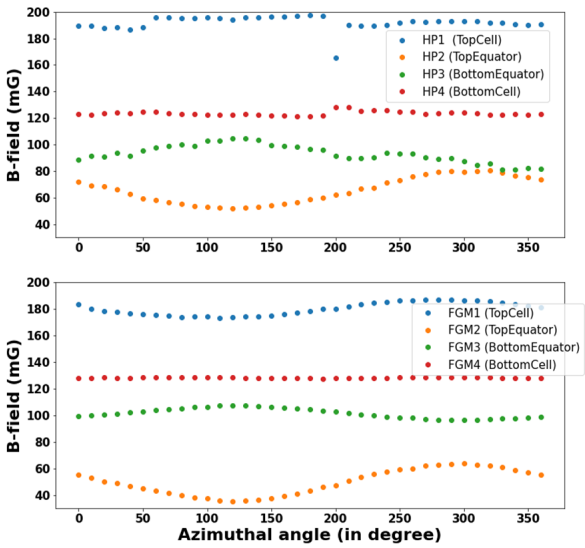

Figure 5: B-field versus azimuthal angle in an ambient magnetic field of ~240 mG at 12 K: (Top) Hall probes reading during scan mode; (Bottom) Fluxgate magnetometers' reading during same scan mode.

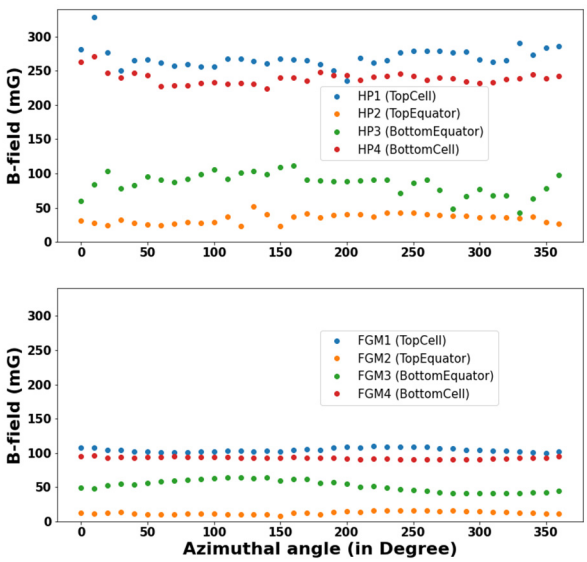

Figure 6: B-field at 4 K and residual field of ~2 mG, after field cooling in ~240 mG external field, versus azimuthal angle: (Top) Hall probes reading during scan mode; (Bottom) Fluxgate magnetometer reading during the same scan.

Another test was done after fast cooldown in an external magnetic field of ~100 mG. Figure 7 shows the magnetic field measured by Hall probe HP4 around the azimuthal position. Once the cavity reached 4.4 K, we kept the external magnetic field as is, and we performed the scan. The same results were obtained four times: after the first test, the cavity was warmed up to 300 K, cooled to ~4 K under the same conditions and a second scan was taken. The test was repeated a third time after removing and re-inserting the test stand in the vertical cryostat, and a fourth time after temperature cycling to 300 K. The cool-down conditions and applied field were the same as for the first scan.

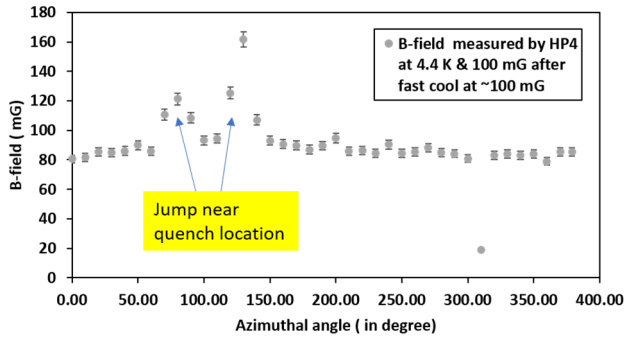

Figure 7: B-field measured at 4.4 K by HP4 along a circumference around the cavity after fast-cool-down in a residual field of ~100 mG.

DISCUSSION

MFSS was able to detect the transition from normal conducting state to superconducting state of Nb cavity as shown in Figs. 3 and 4. From Fig. 6, we see that the trapped flux readings measured by the fluxgate magnetometers are lower in comparison to the Hall probes reading. This discrepancy could be due to the inability of fluxgate magnetometer to measure all trapped flux. Since the fluxgate magnetometer was not able to detect all trapped flux on the cavity surface, we started to look for alternate magnetic sensor. We did some study on anisotropic magneto-resistive sensors [10]. From Fig. 7, we see a magnetic flux jump at ~100° azimuthal position. This flux jump location is very close to the quench location we observed during temperature map as shown in Fig. 8. Thus, we can say that the quench observed during temperature maps could be due to the trapped magnetic flux.

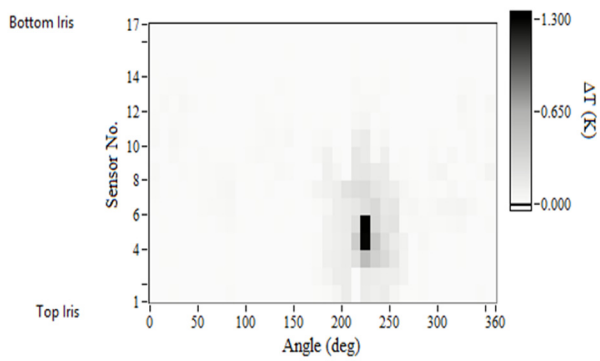

Figure 8: Temperature map of cavity PJ1-1 during quench at 2 K. The origin of the azimuthal angle in the T-map system was shifted by ~120° compared to the origin of the azimuthal angle in the MFSS.

SUMMARY AND OUTLOOK

We have successfully commissioned the magnetic field scanning system at cryogenic temperatures. Initial results show that:

- we could detect the transition from normal conducting state to superconducting state of a Nb cavity.
- Nearly uniform flux-trapping along the cavity circumference was measured after slow field-cooling.

ISBN: 978-3-95450-233-2 ISSN: 2673-5504 doi:10.18429/JACoW-SRF2021-SUPFDV015

- Localized trapped flux after fast field-cooling was detected reproducibly by one of the Hall probe sensors, near the location where the cavity quenched during a previous high-power RF test, with temperature mapping.

We are planning to install eight Hall probes in one bracket and eight anisotropic magneto-resistive sensors in another bracket of MFSS to further increase the spatial coverage of the cavity surface. Several magnetic scanning tests along with high-power RF tests for a cavity with different treatments are planned for future.

ACKNOWLEDGEMENTS

We would like to acknowledge the technical support by the SRF staff, and the machine shop staff at Jefferson Lab.

REFERENCES

[1] F. Furuta *et al.*, "Experimental comparison at KEK of high gradient performance of different single cell superconducting cavity designs," in *Proc. EPAC'06*, Edinburgh, UK, June 2006, paper MOPLS084, pp. 750-752.

[2] W. Singer *et al.*, "Development of large grain cavities," *Phys. Rev. Spec. Top. Accel. Beams*, vol. 16, p. 012003, 2013. doi:10.1103/PhysRevSTAB.16.012003

[3] C. Vallet *et al.*, "Flux trapping in superconducting cavities," in *Proc. EPAC'92*, Berlin, Germany, Mar. 1992, pp. 1295-1298.

[4] H. Padamsee, J. Knobloch and T. Hays, *RF Superconductivity for Accelerators.* New York, NY, USA:Wiley & Sons, 1998.

[5] A. Romanenko *et al.*, "Dependence of the residual surface resistance of superconducting radio frequency cavities on the cooling dynamics around T_c," *J. Appl. Phys.*, vol. 115, iss. 18, p. 184903, 2014. Doi:10.1063/ 1.4875655

[6] Pashupati Dhakal and Gianluigi Ciovati, "Effect of cool-down and residual magnetic field on the performance of niobium-copper clad superconducting radio-frequency cavity," *Supercond. Sci. Technol.*, vol. 31, p. 015006, 2018. doi:10.1088/1361-6668/aa96f5

[7] B. Schmitz *et al.*, "Magnetometric mapping of superconducting RF cavities," *Rev. Sci. Instrum.*, vol. 89, no. 5, p. 054706, 2018. doi:10.1063/1.5030509

[8] T. Okada *et al.*, "Development of temperature and magnetic field mapping system for superconducting cavities at KEK," in *Proc. SRF'19*, Dresden, Germany, Jun.-Jul. 2019, pp. 583-585. doi:10.18429/JACoW-SRF2019-TUP060

[9] I.P. Parajuli *et al.*, "Design and commissioning of a magnetic field scanning system for SRF cavities," in *Proc. SRF'19*, Dresden, Germany, Jun.-Jul. 2019, pp. 547-549. doi:10.18429/JACoW-SRF2019-TUP052

[10] I. P. Parajuli *et al.*, "Evaluation of anisotropic magnetoresistive (AMR) sensors for a magnetic field scanning system for SRF cavities," in *Proc. IPAC'21*, Campinas, Brazil, May 2021, pp. 2304-2307. doi:10.18429/JACoW-IPAC2021-TUPAB344